Tabletop Bremsstrahlung X-Ray Holography: Making Multiwavelength X-Ray Holograms

S. G. Bompadre,* T. W. Petersen, and L. B. Sorensen
Department of Physics, University of Washington, Seattle, Washington 98195-1560
(Received 2 December 1998)

We have used a tabletop x-ray holography apparatus to measure the bremsstrahlung x-ray intensity distribution produced by electron bombardment of a single crystal Ag anode over a far-field hemisphere to parts in 10^4. Using simple computer analysis, we have holographically reconstructed the image of the atoms without the need for detailed crystallographic modeling. We have successfully imaged the silver atoms using both 27.6 and 19.6 keV bremsstrahlung photons.

PACS numbers: 61.10.–i, 07.85.–m, 42.40.–i, 61.14.Nm

Dennis Gabor's dream was to holographically image atoms with an external source of electrons produced using an electron microscope to focus the electrons down to a very small region in front of the sample [1]. Gabor's dream has never been fully realized because the quality of the best electromagnetic lenses is only about as good as the quality of a raindrop is for imaging visible light [2]. However, his dream has been partially realized over the past ten years using electrons produced from a very small region inside the sample as the reference wave [3]. In principle, much better holographic images can be made using x rays instead of electrons [4]. Recently, two forms of internal reference wave x-ray holography have been realized [5,6]. In this Letter, we present a third: multiwavelength bremsstrahlung x-ray holography.

The basis of bremsstrahlung x-ray holography is simple: when bremsstrahlung x-ray photons are produced inside a single crystal sample, the resulting far-field intensity pattern is a Gabor hologram [7]. The holographic reference amplitude is provided by the bremsstrahlung photons which travel directly (without scattering) to the detector, and the holographic object amplitude is provided by the bremsstrahlung photons which undergo single elastic scattering (by the object atoms) on their way to the detector. Since these two final states are indistinguishable, the direct and indirect amplitudes interfere to form a holographic interference pattern. Simple Fourier analysis can be used to reconstruct the image of the atoms around the source atom from this interference pattern.

Bremsstrahlung x-ray holography is attractive for four reasons: (1) Short wavelength x rays can be produced from low-Z materials, thereby allowing higher spatial resolution than their low-energy characteristic x rays would permit. (2) The bremsstrahlung production cross section is large, allowing the measurement of holograms with a tabletop apparatus. (3) X rays interact very weakly with atoms compared to electrons and thereby avoid the strong multiple-scattering problems present in the electron holographies. (4) The bremsstrahlung spectrum is continuous and, consequently, many holograms can be made simultaneously at different photon energies; these multiwavelength holograms may be combined to produce much better quality reconstructions than single energy holograms [8]. Extensive numerical simulations have demonstrated the feasibility of bremsstrahlung x-ray holography [9].

Figure 1 shows a schematic of the experimental apparatus. A tungsten filament was used to provide electrons which were accelerated toward the single crystal silver anode by a 40 kV bias. The interaction of the electrons with the target atoms produced both characteristic and bremsstrahlung photons. The target and the electron gun were housed in a vacuum enclosure maintained at 10^{-8} torr. The x rays exited the vacuum system through a 0.020 inch thick, semicylindrical beryllium window. The experimental apparatus has been described in detail elsewhere [10].

Although, the x-ray production efficiencies are small (about 10^{-3}), so that most of the electron's energy is converted into heat inside the anode, a modest electron beam current of 10 mA still produces about 6×10^{13} x-ray photons into 4π steradians. A recirculating chiller system was used to flow water at 10 °C across the back side of the sample to prevent overheating, since the electron heating would change the lattice spacing, reduce the amplitude of the holograms, and distort or melt the sample.

We used a silver single crystal to demonstrate and develop bremsstrahlung holography. Silver is an excellent

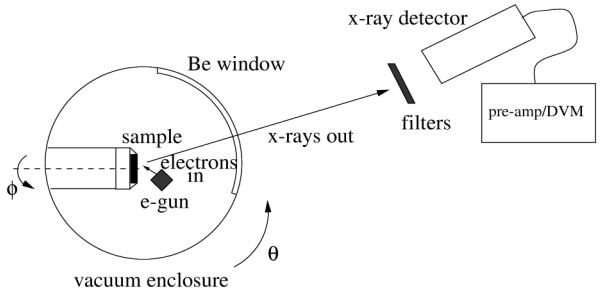

FIG. 1. Schematic of the x-ray holography experimental apparatus. The x rays produced inside the sample exit the vacuum chamber through a beryllium window. They are first energy filtered and then detected. The far-field hemisphere is measured by rotating the crystal 360° about its azimuthal axis ϕ and by rotating the vacuum chamber 90° about its polar axis θ. The detectors remain fixed in space.

electrical and thermal conductor. In addition, silver has a reasonably high melting point (961 °C), and a relatively high atomic number ($Z = 47$). Silver has a face-centered cubic structure with a room temperature lattice constant of $a = 4.0856$ Å. The crystal we used as the anode was a disk 1.5 mm thick and 12 mm in diameter; its surface normal was oriented along the 001 crystal axis to within 0.5°.

The holographic information is contained in the variations of the measured intensities for different outgoing photon directions. As a result, we need two angular degrees of freedom to cover the surface of the far-field sphere. The most convenient way to cover this surface is to rotate the sample inside the vacuum chamber to vary the azimuthal angle ϕ, and to rotate the entire vacuum chamber to vary the polar angle θ.

The photon interference necessary for atomic resolution holography requires sufficiently monochromatic photons. The longitudinal coherence length l_c of the beam is directly related to the energy distribution, $l_c = hc/\Delta E$, and this is approximately the maximum distance over which we will be able to image the neighboring atoms. This issue is particularly important for bremsstrahlung holography, where we need to eliminate the relatively intense characteristic fluorescence radiation, select a narrow energy region from the continuous bremsstrahlung spectrum, and maintain sufficient photon flux for the experiment even after the energy filtering.

To energy filter the bremsstrahlung photons we used balanced Ross filters [11]. The Ross balanced-filter technique uses a combination of two filters made of materials with a small difference in their atomic numbers. This technique relies on the fact that the x-ray absorption coefficients for elements with nearby Z's vary in approximately the same way versus photon energy, except near the absorption edges. If the filter thicknesses are adjusted properly (see Fig. 2), the difference signal will provide a narrow energy bandpass signal. We measure the transmitted beam first through one filter and then through the other filter, and then we take the difference between these two signals.

Two sets of balanced-filter pairs were used: silver and tin provided a passband 3.7 keV wide centered at $E = 27.6$ keV; niobium and molybdenum provided a passband 1.0 keV wide centered at $E = 19.6$ keV. Figure 2 shows the measured signal transmitted through each filter measured with a solid state Si detector, the calculated transmission factor of the filters [12], and the measured difference signal for the Ag/Sn pair. Note that the cancellation is not perfect at low energies and that this will introduce an additional source of noise in the measured hologram. The filters were mounted on a linear translation stage which moved them in and out of the beam under computer control. The x rays were detected using NaI scintillators operated in current mode.

We measured the intensity of the x rays over an entire hemisphere, varying θ and ϕ in 1° steps, from $\theta = 0°$ to $\theta = 90°$, and from $\phi = 0°$ to $\phi = 360°$. With a measuring time of 2.5 sec, about 1.5×10^9 photons per point were detected. Holograms at two different energies were measured simultaneously to allow direct intercomparisons.

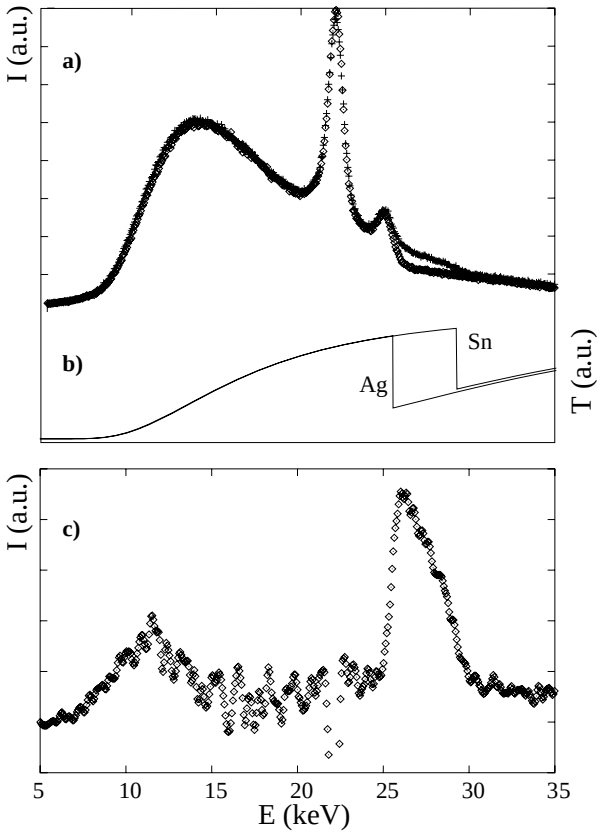

FIG. 2. Operation of the Ross filters measured with a Si detector for the Ag/Sn filter pair. (a) The measured transmission signals. Note that they match well, except in the passband. (b) The calculated energy-dependent transmission factors for the Ag and Sn filters. (c) The measured energy passband for the Ag/Sn pair.

The background was predicted to be uniform and 10^3 times larger than the holographic fringes. To extract the hologram from the measured data—and to correct it for long term fluctuations and sample absorption—we used an area-normalization technique. First, we normalized the data so that curves of constant ϕ had the same integrated area. Then we normalized the (already ϕ normalized) curves of constant θ in the same way. This area-normalization technique very effectively filtered out fluctuations whose time scales were greater than 0.18 mHz. Slow variations in the x-ray intensity due to tungsten deposition on the target, scintillator temperature changes, and barometric pressure changes were all greatly reduced. However, this normalization technique also removed all azimuthally symmetric information from the data, thereby removing all of the interference fringes from atoms along the 001 direction.

The θ and ϕ area-normalized, background-subtracted signal for the data measured using the Ag/Sn filter pair

was about 0.5% of the background level. This was in good agreement with numerical simulations [9]. However, in the case of the Mo/Nb pair, the amplitude of the area-normalized background-subtracted hologram was about 2% of the background. This was larger than the simulations, and indicated additional noise. Fortunately, this extra noise was at different frequencies than the atomic signals, and consequently was separated from the atomic signals by the Fourier filter in the reconstruction algorithm.

To reconstruct the hologram we used Barton's algorithm [13]

$$\psi(\mathbf{r}) = \frac{1}{2\pi R^2} \int \chi(\mathbf{k}) e^{-i\mathbf{k}\cdot\mathbf{r}} \sin\theta \, d\theta \, d\phi$$

to obtain our holographic images of the atoms inside the silver crystal. In this equation, the measured hologram is denoted $\chi(\mathbf{k})$ where $\mathbf{k}$ is the outgoing photon wave vector. To avoid interpolating our data, we used slow Fourier transforms (simple numerical integration) directly on the grid of our data.

Figure 3 shows our reconstructions at different z levels for the hologram measured using the Ag/Sn filters. The reconstruction at $z = 0$ shows four bright spots 4.0 ± 0.2 Å apart in good agreement with the expected value of 4.086 Å. Near the origin there are strong artifacts, which correspond to low spatial frequency noise due to our inability to remove all of the background. The dark spot at the center is related to the area-normalization procedure described above. Some artifacts are also present near the origin in the numerical simulations (see Fig. 5 below), yet these are much weaker and are due to small errors inherent in the single-energy reconstruction technique. The reconstruction at $z = a/2 = 2.043$ Å shows multiple bright spots, most of which do not correspond to atomic images (see below). However, the four spots closest to the center do represent atoms. Their orientation and separation (2.98 ± 0.16 Å) agree with the known structure and known orientation of the crystal in our apparatus. The reconstruction at $z = -a/2$ shows identical features, as expected because of the inversion symmetry with respect to the origin of single-energy holograms. The reconstruction at $z = a = 4.0856$ Å (not shown here) does not show any features corresponding to atoms. Contributions to the interference fringes from atoms farther than the nearest neighbors were too small to be detected due to the limited longitudinal coherence length of the bremsstrahlung photons and the falloff of the reference wave away from the source [9]. Reconstructions at intermediate z levels did not show any features.

Figure 4 shows the same reconstructions for the hologram measured using the Mo/Nb filters. As expected from the narrower passband of this filter pair, these images have better resolution, and the atoms are closer to their expected positions. Other than this, they have essentially the same features as the reconstructions for the Ag/Sn hologram. The $z = 0$ level shows four atoms, 4.1 ± 0.1 Å apart. Again, there are spurious images near the center. The reconstruction at $z = a/2$ clearly shows four atoms separated by 2.87 ± 0.15 Å again in agreement with the known values. As in Fig. 3, there are extra spots that do

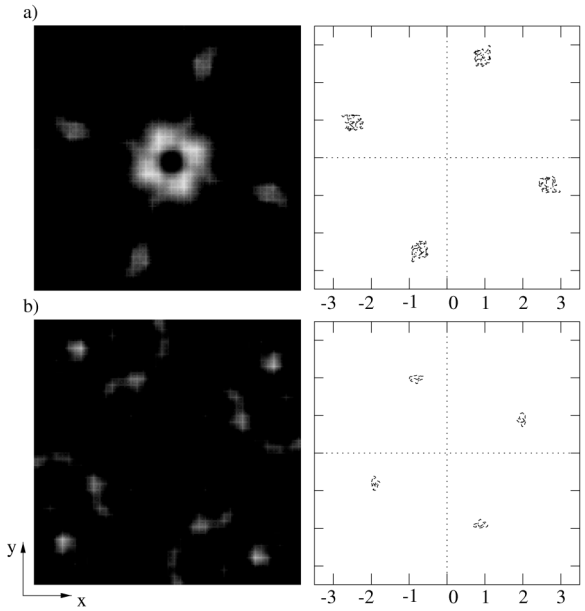

FIG. 3. Reconstructions of the hologram measured with the Ag/Sn filter pair. Each side of the square is 7 Å. (a) Results for the $z = 0$ level. There are four bright atomic images 4.0 ± 0.2 Å apart, and some spurious images near the center. (b) Results for the $z = a/2$ level. The four atoms separated by 2.98 ± 0.16 Å can clearly be distinguished.

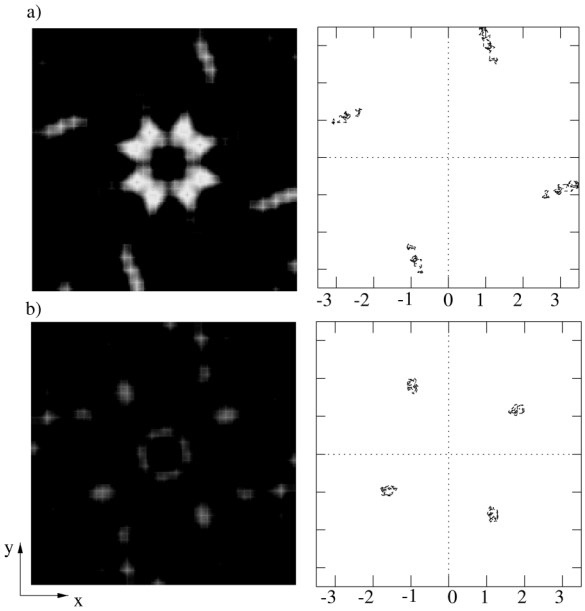

FIG. 4. Reconstructions of the hologram measured with the Mo/Nb filter pair. Each side of the square is 7 Å. (a) Results for the $z = 0$ level. There are four bright atomic images 4.1 ± 0.1 Å apart, and some spurious images near the center. (b) Results for the $z = a/2$ level. The four atoms separated by 2.87 ± 0.15 Å can clearly be distinguished.

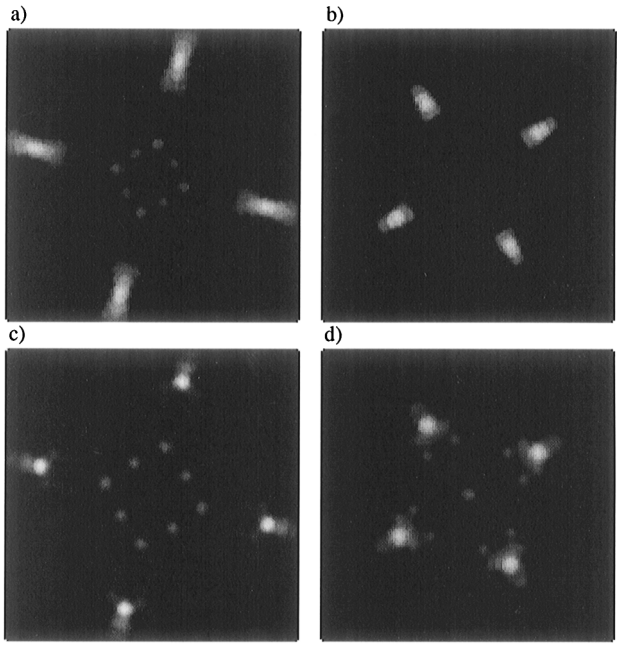

FIG. 5. Reconstructions of the numerically simulated holograms for 22 atom silver clusters [9]. Each side of the square is 7 Å. (a) Reconstruction for the Ag/Sn simulation at $z = 0$. (b) For the Ag/Sn simulation at $z = a/2$. (c) For the Mo/Nb simulation at $z = 0$. (d) For the Mo/Nb simulation at $z = a/2$.

not represent atoms. These are due to noise in the data, and can be safely discarded since they appear at different positions for different x-ray energies.

Figure 5 shows reconstructions of holograms numerically simulated for 22 atom clusters. These simulations included the anisotropic nature of the bremsstrahlung reference wave, the effects of finite energy resolution, the effects of finite angular resolution, and a holographic Debye-Waller factor [9]. Panels 5(a) and 5(b) show the reconstructions for the Ag/Sn pair, and panels 5(c) and 5(d) show the reconstructions for the Mo/Nb pair. These reconstructions agree well with the holographic reconstructions calculated from the data.

In conclusion, we have developed a new technique, bremsstrahlung x-ray holography, to image the atoms inside a crystal. From the measured far-field interference pattern, we have successfully imaged the nearest-neighbor atoms inside a silver crystal using Barton's holographic reconstruction procedure. This work demonstrates the feasibility of this technique to provide atomic structures without detailed modeling.

What is the future of these new x-ray holographies? Will they grow up to be healthy and strong x-ray structural tools? Only time will tell, but it seems clear that great improvements are possible—and will be needed—before these techniques are mature.

We thank Gerald Miller and Dennis Yee for their help during the early stages of this project. We gratefully acknowledge the partial support of this work by the Japanese New Energy and Industrial Technology Development Organization and by the Graduate Research Fund of the University of Washington.

*Current address: Department of Physics, University of Florida, Box 118440, Gainesville, Florida 32611-8440.

[1] D. Gabor, Nature (London) **161**, 777 (1948).
[2] The aberrations of electron lenses cannot be compensated because there are no magnetic monopoles; Maxwell's equations predict only positive aberrations.
[3] For a recent review of electron holography, see C. S. Fadley *et al.*, Prog. Surf. Sci. **54**, 341 (1997).
[4] C. S. Fadley, *Applications of Synchrotron Radiation Techniques to Materials Science*, MRS Symposia Proceedings No. 307 (Materials Research Society, Pittsburgh, 1993).
[5] M. Tegze and G. Faigel, Nature (London) **380**, 49 (1996).
[6] T. Gog *et al.*, Phys. Rev. Lett. **76**, 3132 (1996).
[7] G. A. Miller and L. B. Sorensen, Phys. Rev. B **56**, 2399 (1997).
[8] J. J. Barton, Phys. Rev. Lett. **67**, 3106 (1991).
[9] S. G. Bompadre, Ph.D. dissertation, University of Washington, 1998.
[10] T. W. Petersen, Ph.D. dissertation, University of Washington, 1997.
[11] P. Kirkpatrick, Phys. Rev. **10**, 186 (1939).
[12] W. H. McMaster *et al., Compilation of X-ray Cross Sections*, Lawrence Radiation Laboratory Report UCRL-50174 (National Bureau of Standards, Springfield, Virginia, 1969).
[13] J. J. Barton, Phys. Rev. Lett. **61**, 1356 (1988).